Gene Therapy With the Caspase Activation and Recruitment Domain Reduces the Ocular Inflammatory Response

Cristhian J Ildefonso[1], Henrique Jaime[2], Manas R Biswal[1], Shannon E Boye[3], Qiuhong Li[3], William W Hauswirth[3] and Alfred S Lewin[1]

[1]Department of Molecular Genetics & Microbiology and Powell Gene Therapy Center, University of Florida College of Medicine, Gainesville, Florida, USA; [2]Department of Biology, University of Florida College of Liberal Arts & Sciences, Gainesville, Florida, USA; [3]Department of Ophthalmology and Powell Gene Therapy Center, University of Florida College of Medicine, Gainesville, Florida, USA

Inflammation is a key component of chronic and acute diseases of the eye. Our goal is to test anti-inflammatory genes delivered by an adeno-associated virus (AAV) vector as potential treatments for retinal inflammation. We developed a secretable and cell penetrating form of the caspase activation and recruitment domain (CARD) from the apoptosis-associated speck-like protein containing a CARD (ASC) gene that binds caspase-1 and inhibits its activation by the inflammasome. The secretion and cell penetration characteristics of this construct were validated *in vitro* by measuring its effects on inflammasome signaling in a monocyte cell line and in an retinal pigmented epithelium (RPE) cell line. This vector was then packaged as AAV particles and tested in the endotoxin-induced uveitis mouse model. Gene expression was monitored one month after vector injection by fluorescence fundoscopy. Ocular inflammation was then induced by injecting lipopolysaccharide into the vitreous and was followed by enucleation 24 hours later. Eyes injected with the secretable and cell penetrating CARD AAV vector had both a significantly lower concentration of IL-1β as well as a 64% reduction in infiltrating cells detected in histological sections. These results suggest that anti-inflammatory genes such as the CARD could be used to treat recurring inflammatory diseases like uveitis or chronic subacute inflammations of the eye.

Received 13 June 2014; accepted 10 February 2015; advance online publication 17 March 2015. doi:10.1038/mt.2015.30

INTRODUCTION

Chronic inflammation is a contributing factor to a variety of diseases from asthma to Alzheimer disease. Activation of a cytoplasmic signal transduction complex called the NLRP3 inflammasome is integral to chronic inflammation in most tissues. Inflammasome signaling has been implicated in the pathogenesis of chronic ocular diseases including diabetic retinopathy[1] and age-related macular degeneration[2] as well as in recurrent ocular inflammations such as uveitis.[3] This signaling complex induces the activation and secretion of the proinflammatory cytokine interleukin-1β (IL-1β). Pro-interleukin-1β is processed into its active form by caspase-1, which in turn, is activated by the inflammasome. Within this complex, the engagement of the NLRP3 receptor leads to its recruitment of the ASC (apoptosis-associated speck-like protein containing a caspase recruitment domain) through a pyrin–pyrin domain interaction. ASC then binds the proenzyme caspase-1 through a caspase activation and recruitment domain (CARD)-CARD interaction. The recruited pro-caspase-1 self-cleaves into its active form. The potent inflammatory cytokines IL-1β and IL-18 are then cleaved into their active forms by caspase-1 and secreted into the extracellular space. These mechanisms have been reviewed elsewere.[4–6] These cytokines mediate many inflammatory processes by binding to their respective cellular receptors upon secretion. The IL-1β receptor is expressed in glial cells[7] and in retina pigment epithelium cells,[8] but also in neuronal cells and retina endothelial cells.[9] However, the expression of IL-18 receptor within the cells of the retina has not been described. The importance of IL-1β and IL-18 in inflammation makes the inflammasome pathway a principal target for the development of anti-inflammatory therapies.

The roles of IL-1β in inflammatory diseases and therapies based on the suppression of innate immunity have been intensively studied and are reviewed elsewere.[10] Several groups have tested methods of blocking IL-1β signaling, including antibodies that inhibit its interaction with its cognate receptor.[11] An alternative method currently approved for human use is the IL-1 receptor antagonist (IL-1RA) known as Anakinra.[10,12,13] Both of these methods, however, block the effects of only one of the cytokines regulated by the inflammasome and do not alter signaling mediated by IL-18. This cytokine also has proinflammatory properties that affect the adaptive immune system, specifically the Th1-mediated response.[14] IL-18 plays a role in inflammatory diseases such as colitis,[15,16] arthritis,[17] and myocardial dysfunction.[18,19] Protein therapy with anticytokine antibodies or with receptor antagonists would require repeated injections to control a chronic inflammation. Furthermore, unless combined, each therapy would only control one aspect of the inflammatory process. We therefore hypothesize that by targeting the processing of procaspase-1, we could develop a therapy that would block the

Correspondence: Alfred S Lewin, Department of Molecular Genetics & Microbiology, University of Florida College of Medicine, 1200 Newell Drive, PO Box 100266, Gainesville, Florida 32610-0266, USA. E-mail: lewin@ufl.edu

production of both IL-1β and IL-18. By using virus-based delivery of a secreted inhibitor one could avoid repeated injections of protein inhibitors.

Endotoxin-induced uveitis (EIU) is commonly used to model acute ocular inflammation.[20] In this model, an acute inflammatory response is induced within the anterior chamber and vitreous of the animal by an intravitreal injection of lipopolysaccharide.[21] The inflammatory response peaks at 24 hours post-lipopolysaccharide (LPS) injection and resolves within 48 hours. Within 16 hours, cytokines such as IL-1 and IL-6 reach peak levels within the eye. However, at 24 hours, the most prominent cytokines are interferon (IFN)-γ and IL-10.[22] This model is also characterized by the recruitment of granulocytes and monocytes into the anterior and vitreous chamber.[23] Therefore, this makes an excellent model for the evaluation of anti-inflammatory therapies for use within the eye.

In this study, we developed a secretable and cell penetrating version of the ASC CARD domain that can be delivered by an AAV vector. We characterized its anti-inflammatory effects in cell culture models of inflammation. Finally, we used a mouse model of acute uveitis to study the effect of this anti-inflammatory vector *in vivo*. Although we tested this vector in an ocular disease model, it could be of potential benefit when studied in diseases of other tissues where the inflammasome activation is involved.

RESULTS

The CARD domain of ASC is an inhibitor of IL-1β secretion

To investigate the role of caspase-1 on the development of IL-1β secretion, we generated cells stably expressing the CARD domain from the ASC gene (a.a. 105–195) using a lentiviral vector. We also fused the HIV-derived Tat-peptide that has been shown to provide cell-penetrating properties to it fusion partner[24] to the CARD domain (**Figure 1a**). Within the retina are several cell types that could be the source of IL-1β, including Müller glia, microglia, and the retinal pigmented epithelium (RPE). We used the THP-1 human monocytic cell line and the human RPE-derived cell line ARPE-19 to generate cell lines stably expressing the CARD or the TatCARD constructs. The effect of both CARD and TatCARD expression on IL-1β and IL-18 was determined by challenging THP-1 cells transduced with CARD, TatCARD or with the empty lentiviral vector (**Figure 1b** inset) with IFN-γ in the presence or absence of LPS. In these cells, there was an increase in IL-1β and IL-18 secretion among cells transduced with the empty vector that was significantly inhibited in cells expressing either CARD or the TatCARD construct (**Figure 1b**). These results demonstrate that the expression of CARD can inhibit the LPS induced IL-1β and IL-18 secretion, and that its fusion with the Tat peptide does not affect this property. To verify that this inhibitory effect of TatCARD was not cell-specific or LPS-specific, ARPE-19 cells transduced with either TatCARD or with empty lentiviral vector were challenged with 4-hydroxynonenal (4-HNE). This molecule is a reactive aldehyde produced during increases in oxidative stress in the retina. 4-HNE has been shown to induce the secretion of IL-1β by RPE cells,[25] possibly by interaction with TLR-4 (ref. [26]). Although 4-HNE was capable of inducing the secretion of IL-1β in ARPE-19 cells (**Figure 1c**, checked bars), the expression of TatCARD was sufficient to block this secretion (**Figure 1c**, black bars). When we immunoprecipitated the lysate from ARPE-19 cells stably transfected with our TatCARD construct using anti-caspase-1 antibody, the band corresponding to the TatCARD fusion protein coprecipitated (**Figure 1d**) suggesting that TatCARD binds to caspase-1 even in the absence of an inflammasome signaling activator. Taken together, these results confirm that TatCARD is an inhibitor of IL-1β secretion in both monocyte-like and RPE-like cells.

Development of a secretable and cell penetrating CARD

In order to block the secretion of IL-1β in the retina, our vector must either transduce all the different cell types in the retina that can secrete this cytokine or demonstrate a by-stander effect, so that transduced cells serve as a source of secreted protein that can block IL-1β processing in neighboring cells (**Figure 2a**). We developed a secretable form of our TatCARD by fusing its amino terminus to a green fluorescent protein (GFP) sequence containing the secretion signal from the immunoglobulin kappa chain, using a furin cleavage site between the GFP sequence and TatCARD (**Figure 2b**). This construct was based on a similar plasmid designed to deliver an Ang-1–7 peptide.[27] This fused molecule named sGFP-TatCARD was cloned in a lentiviral vector plasmid under the control of elongation factor 1 (EF1) promoter and was packaged as lentiviral particles (**Figure 2c**). The sGFP-TatCARD molecule is expected to be secreted via the endoplasmic reticulum and golgi and, therefore, to show a punctate distribution by fluorescence microscopy, in contrast to the soluble GFP which displays a cytoplasmic accumulation. To test this property of our construct, we transduced HEK293T cells with lentiviral particles delivering either GFP or the sGFP-TatCARD construct, and stably transduced cells were selected with puromycin. Because the puromycin resistance gene (puroR) was directly linked to the expression of our transgene through the 2A self-cleaving peptide, any puromycin-resistant cell also expressed the sGFP-TatCARD transgene. When these cells were imaged by fluorescence microscopy, we observed the characteristic cytoplasmic distribution of GFP, but the sGFP-TatCARD construct showed a distinct punctate pattern (**Figure 2d**) suggesting that the sGFP-TatCARD fusion protein was targeted for secretion.

Adeno-associated virus (AAV) has been widely used for ocular gene therapy in both animal models and human clinical trials. Because of its record of safety and efficacy,[28] we decided to reclone our construct into an AAV plasmid (**Figure 3a**). This plasmid contains a CMV enhancer-chicken β-actin promoter with a shortened intron (smCBA), which is known to be constitutively active in the retina tissue.[29] HEK293T cells were transiently transfected with the AAV plasmids delivering either GFP or sGFP-TatCARD under the control of this promoter. To detect the presence of either sGFP-TatCARD or TatCARD by western blot, we used an antibody that recognizes the amino acids 182–195 of the human ASC protein, a portion of the CARD domain of this molecule. When the conditioned media of the transfected cells were harvested, we detected the expression of both the sGFP-TatCARD (~42 KDa) and the proteolyzed TatCARD (~15 KDa) species (**Figure 3b**). There

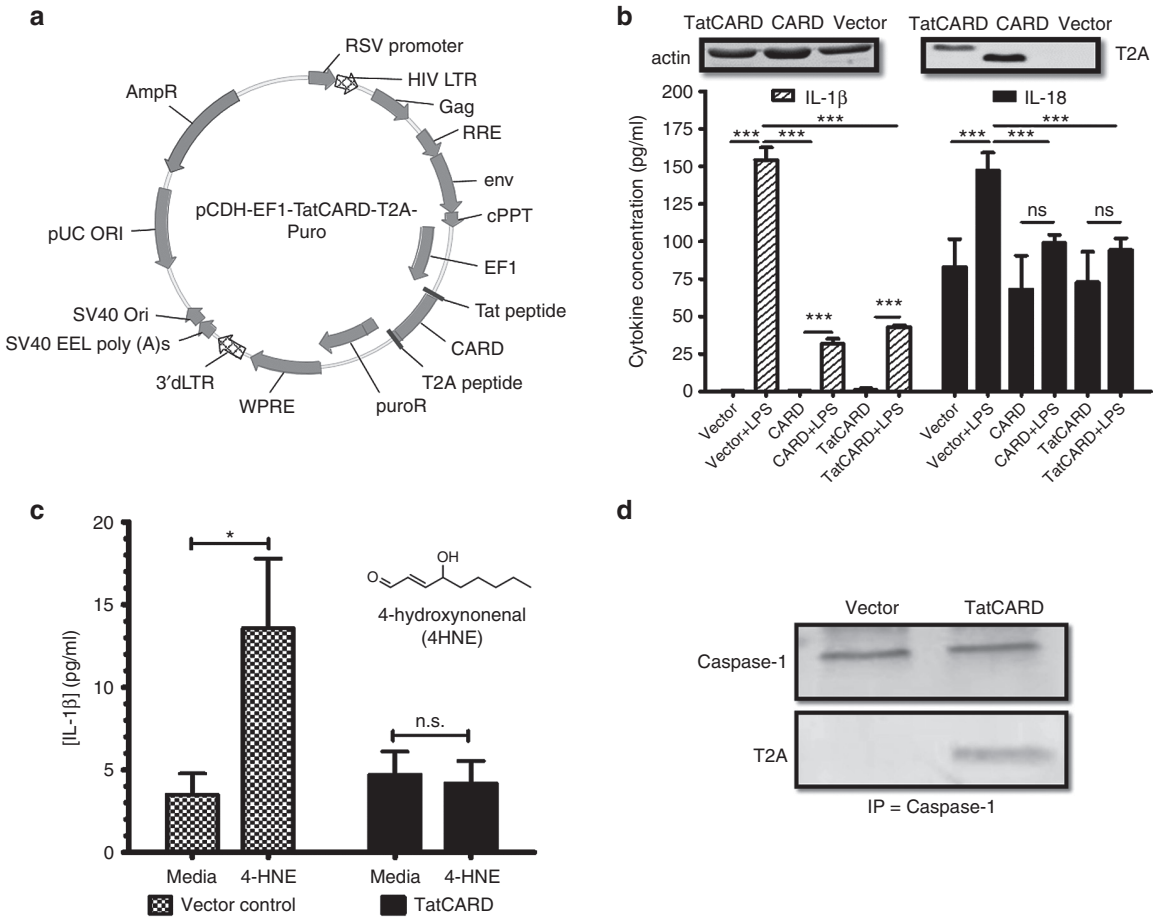

Figure 1 The CARD domain from the ASC gene is an inhibitor of caspase-1. (**a**) Lentiviral vector plasmid delivering the TatCARD gene construct. AmpR, ampicillin resistance gene; cPPT, central polypurine tract; EF1, elongation factor-1; HIV LTR, human immunodeficiency virus long terminal repeat; Ori, origin of replication; puroR, puromycin resistance gene; RRE, Rev response element; RSV, Rous sarcoma virus; SV40, simian virus 40; WPRE, woodchuck hepatitis virus post-transcriptional regulatory element. (**b**) Expression of CARD inhibits the lipopolysaccharide (LPS)-induced secretion of interleukin (IL)-1β and IL-18 from THP-1 cells. THP-1 cells were transduced with lentiviral vectors delivering either puroR, CARD-puroR, or TatCARD-puroR and selected with puromycin. Stably transfected cells were primed with IFN-γ (10 ng/ml) and then challenged with LPS (10 µg/mL) for 18 hours in serum-free media. The concentration of secreted cytokines was quantified by enzyme-linked immunosorbent assay (ELISA). n.s., not significant. (**c**) Expression of TatCARD inhibits the secretion of IL-1β in an *in vitro* model of RPE inflammation. ARPE-19 stably expressing puroR or TatCARD were generated as in **b** and challenged with 4-HNE (30 µmol/l). The concentration of secreted IL-1β was quantified by ELISA. (**d**) The CARD domain of the ASC gene binds to caspase-1. Protein lysates from ARPE-19 cells stably expressing either the puroR or the TatCARD-puroR were subjected to caspase-1 immunoprecipitation. Immunoprecipitated samples were then separated by SDS-PAGE in a 12% gel and transferred into a polyvinylidene fluoride (PVDF) membrane. Membranes were probed with either anti-caspase-1 antibody or anti-T2A antibody (to detect TatCARD). Graphed values represent average ± SD, $n = 3$. CARD, caspase activation and recruitment domain.

was no CARD positive protein in the conditioned media of GFP-transfected cells although we loaded the same amount of protein. These results demonstrate that the sGFP-TatCARD fusion protein could be both secreted and proteolyzed into GFP and TatCARD.

The last step of the by-stander effect is the penetration of nonexpressing cells by the released TatCARD present in the conditioned media. To determine if the secreted TatCARD could enter nontransfected cells, the conditioned media from cells transfected with either GFP or sGFP-TatCARD was overlaid on nontransfected ARPE-19 cells which were then induced to secrete IL-1β by treatment with 4-HNE. Treatment with TatCARD-conditioned medium significantly reduced IL-1β secretion compared to ARPE19 cells exposed to conditioned media from GFP-transfected cells (**Figure 3c**). Taken together, these results demonstrate that we created a secretable and cell-penetrating TatCARD protein.

Validation of an AAV vector delivering the secretable and cell penetrating CARD in the EIU mouse model

To test our secretable TatCARD construct *in vivo*, the sGFP-TatCARD plasmid was packaged using a helper plasmid that encoded an AAV capsid containing four tyrosine-phenylalanine (Y-F) and one threonine-valine (T-V) mutation on its surface. This AAV2(quadY-F+T-V) variant infects multiple retinal cell types when delivered intravitreally.[30] We injected C57BL/6J mice with our AAV2(quadY-F+T-V) vector delivering GFP in one eye or sGFP-TatCARD in the contralateral eye. To control for the effects of injecting the eye, we sham injected some of the animals with sterile saline. Two weeks after the injection, we evaluated the effects of the vectors on the light-response of the retina by electroretinography (ERG). We found no significant differences between eyes that received AAV GFP, AAV sGFP-TatCARD, or sham injection in the average amplitudes of the

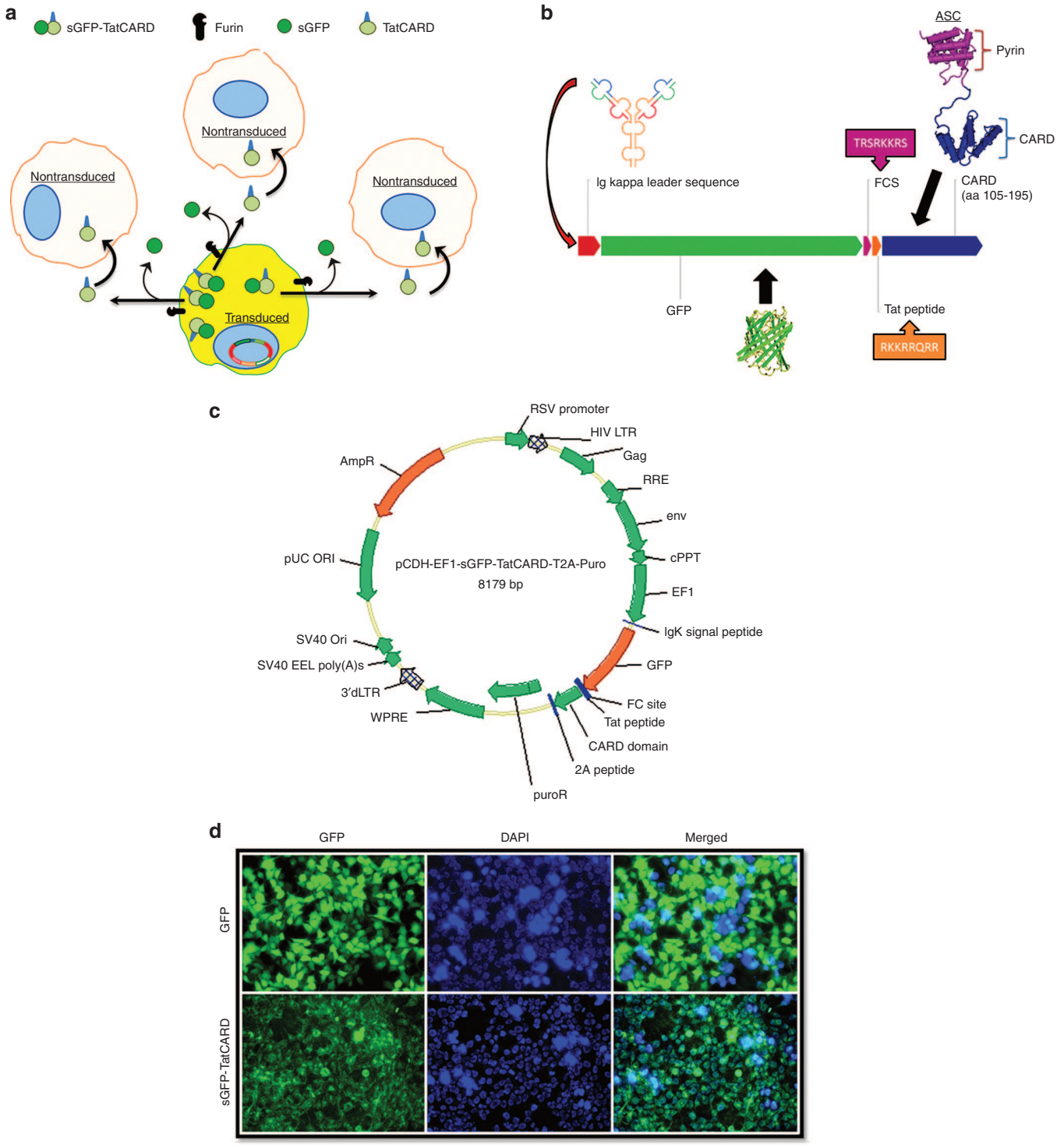

Figure 2 Development of a secretable and cell penetrating CARD construct. (**a**) Hypothetical model of the sGFP-TatCARD by-stander effect. A virally transduced cell will express the sGFP-TatCARD protein and will target it for secretion. Upon reaching the cell membrane, furin will cleave its substrate sequence in the sGFP-TatCARD causing the separation of sGFP from TatCARD. The now extracellular and free form of TatCARD will penetrate nearby cells due to the presence of the Tat peptide. (**b**) Detailed map of sGFP-TatCARD indicating the sources of its components. The secretion signal is derived from the Igκ leader sequence. GFP is a humanized version of green fluorescent protein. FCS is the furin cleavage site, which substrate for the cellular protease furin. Tat is the 8-residue cell penetrating peptide derived from the *tat* gene of HIV-1. CARD 105–195 is the caspase-1 binding domain of the ASC protein. Together these component result in a secreted (Igκ) protein that can be tracked following transduction (GFP), separated from its carrier protein by furin (FCS) and enabled to penetrate neighboring cells (Tat), where it can inhibit the activation of caspase 1 (CARD). (**c**) Map of the lentiviral vector plasmid pCDH-EF1-sGFP-TatCARD. The sGFP-TatCARD construct was cloned between the EF1 promoter and the T2A sequence in frame with the puroR gene sequence. To allow the transcription of the sGFP-TatCARD and the puroR as a single mRNA, the stop codon of the sGFP-TatCARD construct was deleted. (**d**) The sGFP-TatCARD has a punctate cellular distribution *in vitro*. HEK293T cells were transduced with lentiviral vectors delivering either GFP or sGFP-TatCARD and selected with puromycin. Cell nuclei were stained with 4′,6-diamidino-2-phenylindole (DAPI) in cells grown on a six-well plate. Expression and distribution of GFP was determined in viable cells by fluorescence microscopy. CARD, caspase activation and recruitment domain.

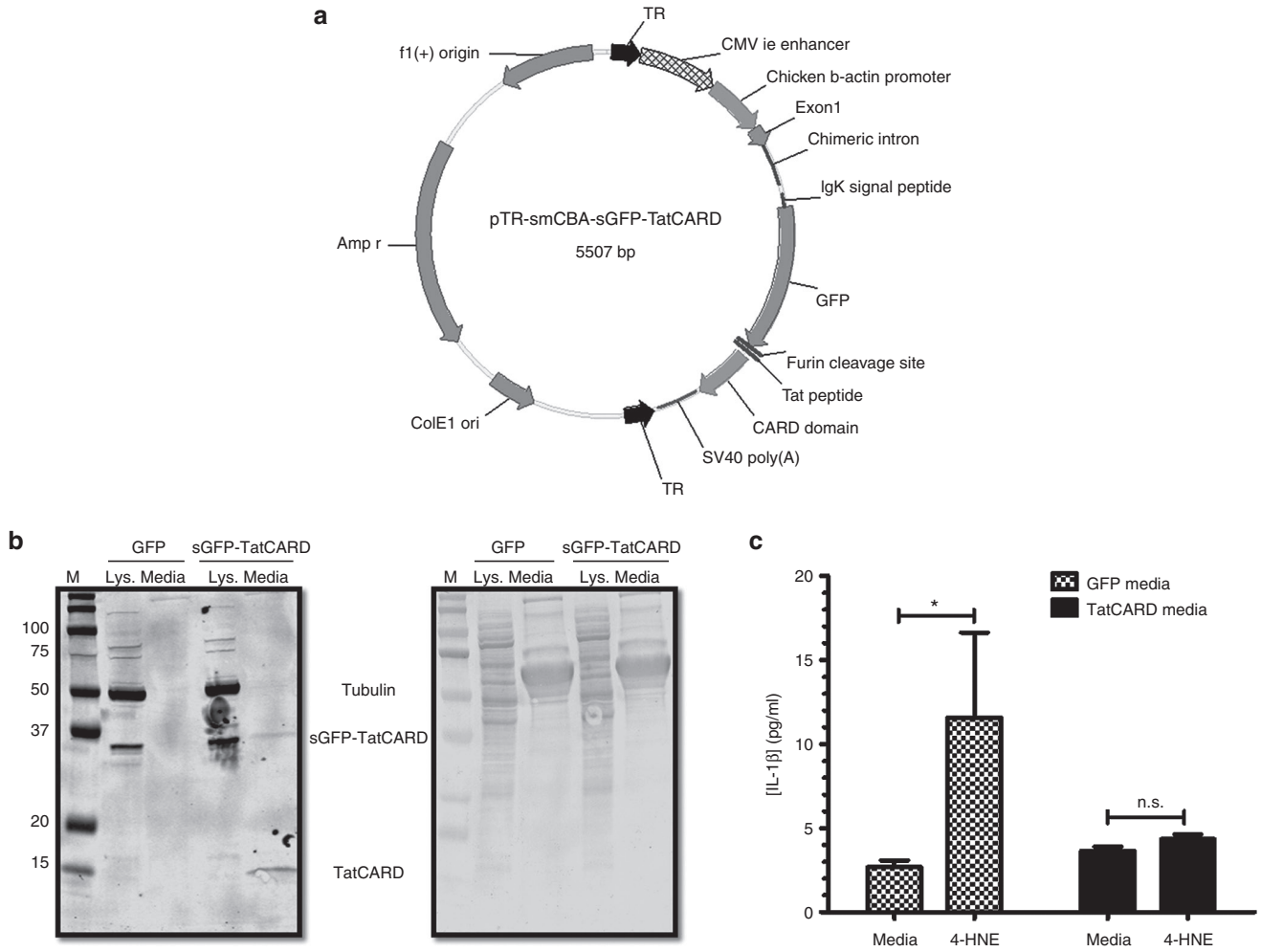

Figure 3 Validation of the secretable and cell penetrating CARD construct. (**a**) Map of an AAV plasmid delivering the sGFP-TatCARD construct. The TatCARD construct was cloned in an AAV plasmid between the smCBA promoter and the SV40 poly A signal. TR, terminal repeat sequences of AAV2. (**b**) The TatCARD gene product is secreted by transfected cells. HEK293T cells were transiently transfected with AAV plasmids expressing either GFP or sGFP-TatCARD under the control of the smCBA promoter. The conditioned media from these cells was concentrated, and the presence of TatCARD was evaluated by immunoblot. Total protein was detected by amido black staining of the membrane. (**c**) The biological activity of TatCARD can be transferred *in vitro*. Conditioned media from cells transfected with either GFP or sGFP-TatCARD expressing plasmid was overlaid on ARPE-19 cells. These cells were then stimulated with 4-HNE, and the concentration of secreted IL-1β in the media was measured by ELISA. Graphed values represent average ± SEM, $n = 5$. CARD, caspase activation and recruitment domain.

a-wave (indicative of photoreceptor activity), the b-wave (indicative of the bipolar cell activity), or the c-wave (indicative of the RPE activity) (**Figure 4a**). We further validated the safety of the TatCARD vector by evaluating the retina morphology by spectral domain optical coherence tomography (SD-OCT). Using this technique, we found no difference in retinal structure among the three treatment groups (sham, GFP, and sGFP-TatCARD) (**Figure 4b**). Using imaging software, we quantified the thickness of each of the retina layers, and did not observe any differences among the different groups (**Table 1**). The ERG and SD-OCT results suggest that the intravitreal delivery of our sGFP-TatCARD vector is safe.

Three weeks after the injection, the expression of GFP was detected by fluorescence fundoscopy (**Figure 5a**,**b**). As expected, the eyes injected with AAV vector delivering GFP showed a distinct labeling of the retina cells, characteristic of transduced retinal ganglion cells. However, the eyes injected with the sGFP-TatCARD vector demonstrated a diffused expression of GFP as expected of a secreted GFP (**Figure 5b**). This diffused GFP signal was not observed in noninjected eyes ruling out a signal from autofluorescene.

Next, we investigated the effect of expressing the sGFP-TatCARD on the LPS induced secretion of IL-1β. Intravitreal injection of LPS is a widely accepted model of acute uveitis, an inflammation of ocular tissues that may be of infectious or autoimmune origin.[31–37] We injected AAV-sGFP-TatCARD injected mice 1 week after their fundus evaluation with 25 ng of LPS (intravitreally) and harvested their vitreous 24 hours later to study the effect of TatCARD expression on the levels of IL-1β. The levels of IL-1β were lower in vitreous samples from eyes treated with TatCARD when compared with eyes treated with GFP or sham injected (**Figure 5c**). These results suggest that, as in the *in vitro* experiments, the expression of our TatCARD construct inhibited the caspase-1 activation of IL-1β.

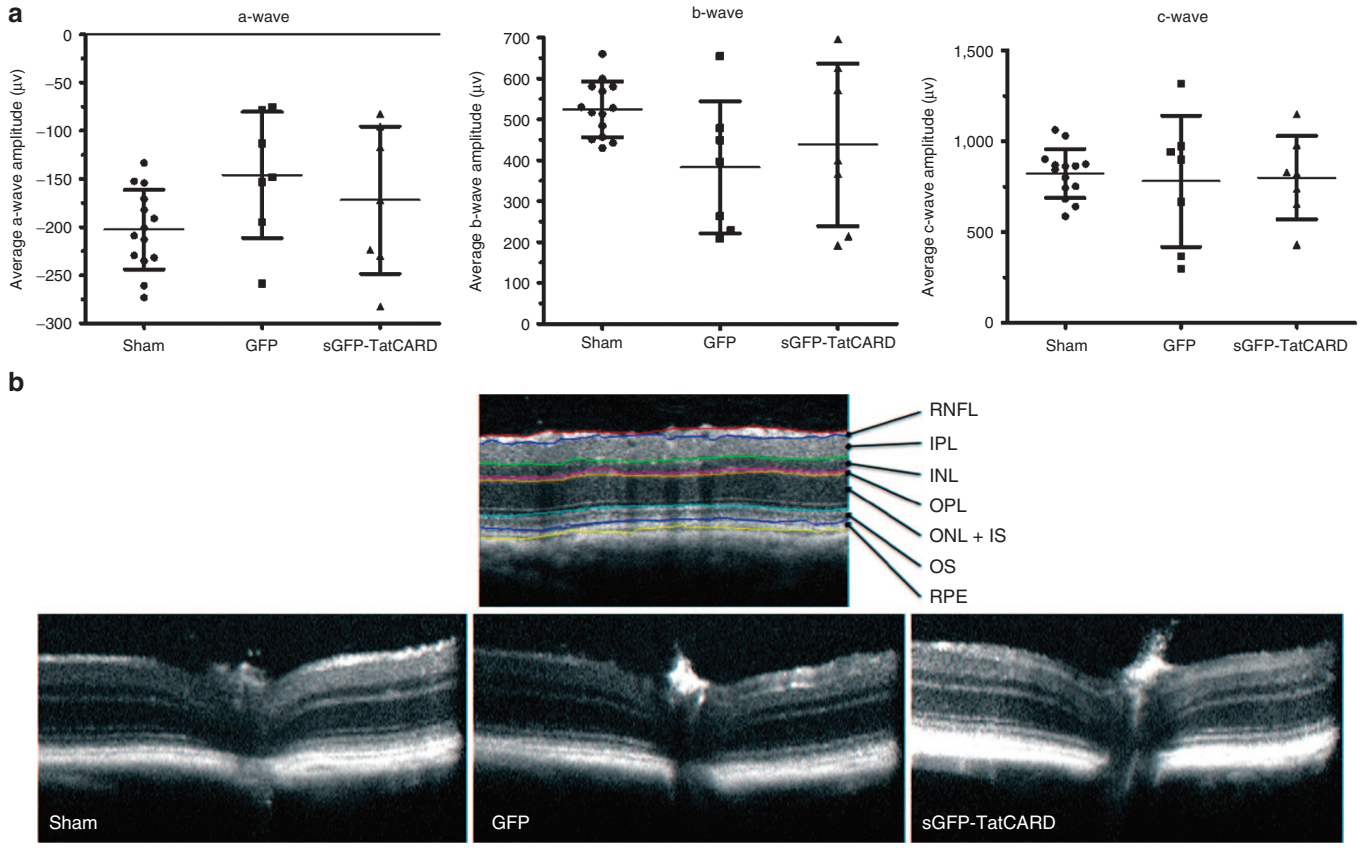

Figure 4 Intravitreal delivery of TatCARD gene product does not alter retinal structure or function. (**a**) AAV2(quadY-F+T-V)/smCBA-sGFP-TatCARD injection into the vitreous chamber does not affect the electrical activity of the retina. C57BL/6J mice were injected intravitreally with 3×10^9 vector genomes of AAV delivering either GFP or sGFP-TatCARD. As a control, some mice received a sham injection. Three weeks after the injection, mice were evaluated by electroretinogram to study the effects of these injections on the retina activity. No significant difference was observed among the treatments in the average a-, b-, or c- wave amplitudes (sham = 14 eyes, GFP = 7 eyes, sGFP-TatCARD = 7 eyes). (**b**) Gene delivery of sGFP-TatCARD intravitreally does not alter the thickness of the retina layers. Mice described above were examined by spectral domain optical coherence tomography (SD-OCT) to determine the effects of the different treatments on the thickness of the different retina layers. A representative B-scan image of each treatment is shown alongside a reference image identifying the different layers of the eye. CARD, caspase activation and recruitment domain.

Table 1 Thickness of retina layers measured by SD-OCT (μm)

Retina nerve fiber layer	11 ± 2	13 ± 2	12 ± 2
Inner plexiform layer	35 ± 6	37 ± 8	31 ± 4
Inner nuclear layer	37 ± 4	37 ± 4	39 ± 4
Outer plexiform layer	9 ± 1	10 ± 1	9 ± 1
Outer nuclear layer + inner segment	83 ± 10	88 ± 7	83 ± 9
Outer segment	27 ± 1	26 ± 1	27 ± 2
Retina pigment epithelium	17 ± 1	17 ± 1	17 ± 1

Although decrease in IL-1β levels demonstrate the biological activity our vector *in vivo*, our long-term goal is to develop this vector into a therapy for inflammatory diseases. We therefore used the EIU mouse model as in the previous experiment but measuring a more clinically relevant endpoint, the number of infiltrating cells. We harvested the eyes of animals that were injected intravitreally with 25 ng of LPS for histological evaluation 24 hours after LPS injection. When evaluated by histology, we observed that eyes treated with the TatCARD had less cellular infiltration in the vitreous body (between the lens and the retina) than either the AAV- GFP injected or the sham-injected eyes (**Figure 6a**). When these cells were quantified by two independent investigators who were unaware of the treatment group, we found that indeed the eyes treated with the TatCARD had a statistically significantly lower number of infiltrating cells within their vitreous body when compared to the GFP or sham control-treated eyes (**Figure 6b**). However, when the cells in the anterior chamber were quantified, we did not find a difference among the different groups (**Figure 6c**). These results suggest that intravitreal injection of the AAV-sGFPTatCARD vector can block the activation of IL-1β and that, by doing so, it can inhibit the recruitment of infiltrating cells induced by LPS within the vitreous body, but not within the anterior chamber.

DISCUSSION

We have developed a secretable and cell penetrating CARD domain that can be delivered as an AAV vector using the secretion signal from the Ig κ-chain gene and the Tat peptide sequence from the HIV Tat protein. This TatCARD protein can bind to caspase-1 and inhibit its processing of IL-1β and IL-18 both *in vitro* and *in vivo*. Using the EIU mouse model, we observed that the expression of

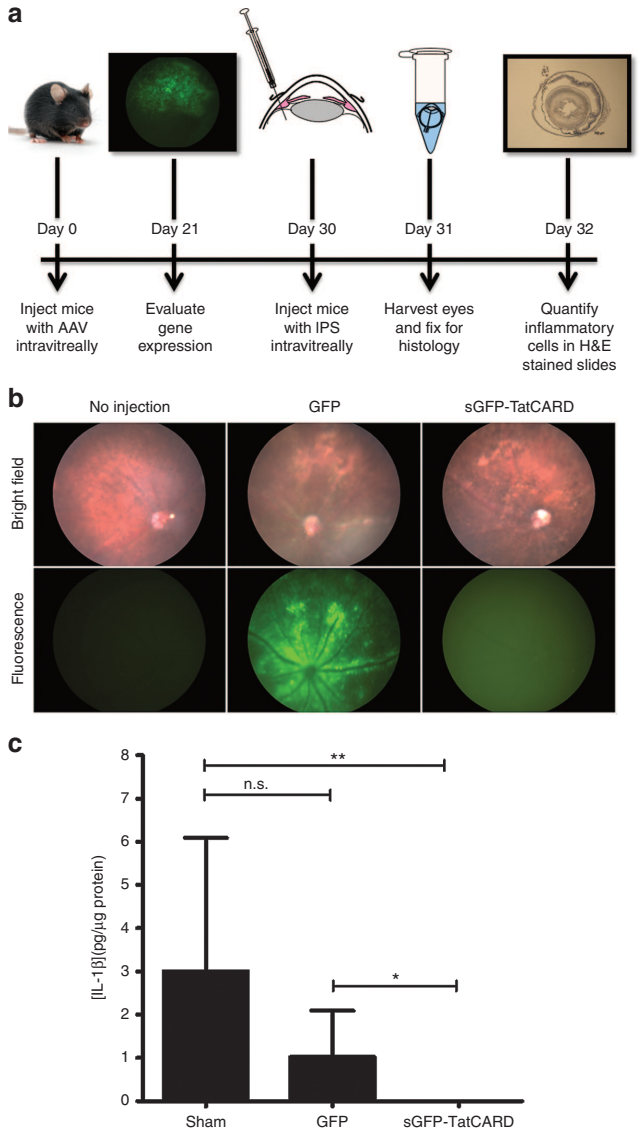

Figure 5 ***In vivo*** **expression of TatCARD gene product inhibits IL-1β secretion.** (**a**) Experimental design for testing the AAV2(quadY-F+T-V)/smCBA-sGFP-TatCARD vector in the endotoxin-induced uveitis mouse model. C57BL/6J mice were injected intravitreally with 3×10^9 vector genomes of AAV2 delivering either GFP or TatCARD. Twenty-one days later, gene expression was determined by fluorescent fundoscopy. Nine days afterwards, mice received 25 ng of lipopolysaccharide (LPS) intravitreally. Eyes were enucleated 24 hours later. (**b**) Fundus of animals injected with AAV vector. Mice were evaluated 21 days after AAV injection by fluorescence fundoscopy. Eyes injected with the AAV-sGFP-TatCARD vector showed a diffused GFP expression representative of secreted GFP. A noninjected eye was used as a negative control. (**c**) Expression of TatCARD reduced the concentration of IL-1β *in vivo*. Vitreous humor was collected from eyes 24 hours after injection of LPS. The concentration of IL-1β in the vitreous humor was measured by ELISA. Eyes injected with the AAV vector delivering the TatCARD gene had statistically significantly lower concentration of IL-1β when compare with samples from eyes injected with the AAV vector delivering GFP or with sham injected eyes. Graphed values represent average ± SD, $n = 6$ eyes per treatment. CARD, caspase activation and recruitment domain.

TatCARD could inhibit the recruitment of infiltrating cells into the vitreous body, but not into the anterior chamber. The lack of flow between these two chambers, and therefore the lack of transfer of TatCARD to the aqueous humour, probably explains the localized effects of our vector. Tsai *et al.*[38] demonstrated that expression of the IL-1Ra from an AAV vector in the eye of rabbits can mitigate endotoxin induced inflammation, thus demonstrating the importance of the IL-1β signaling in the inflammatory process. Our approach has the added value of inhibiting the processing of IL-18 as well, another cytokine activated by the inflammasome. In addition, our approach also has the theoretical advantage of preventing the *production* of IL-1β rather than binding to cytokine that has already been processed and secreted. Our results contrast with those reported by Rosenzweig *et al.*[39] who reported that a germ-line knockout of caspase-1 did not reduce infiltrating cells in the EIU mouse model of uveitis. One potential difference is that we inhibited in caspase-1 activity in adult mice rather than prior to embryonic development. It has been previously reported that the deletion of caspases can result in the upregulation of compensatory caspases.[40]

Caspase-1 is the enzyme responsible for the conversion of the pro-IL-1β into IL-1β. However, this enzyme has also been associated with the regulated cell death process known as pyroptosis.[41] Although we did not explore the effect of our vector on pyroptosis-mediated cell death, we envision conducting this avenue of research using animal models of retina degeneration such as the light-induced model of retinal degeneration. In that model, caspase-1 activation plays an important role in cell death that is independent of IL-1β.[42,43] Increased levels of IL-1β have been reported in diabetic retinopathy[44,45] and in animal models of age-related macular degeneration.[46,47] It would certainly be of interest to test the AAV-TatCARD vector in models of these diseases. We have generated a mouse model of geographic atrophy based on mitochondrial oxidative stress in the RPE, and we will test the ability of AAV-TatCARD to inhibit retinal degeneration in that chronic model.[48]

MATERIALS AND METHODS

Cell culture. The human HEK293T cell line was grown in Dulbecco's modified Eagle's medium supplemented with 10% fetal bovine serum and 1% penicillin-streptomycin (Pen-Strep) solution. The human ARPE-19 cell line was obtained from ATCC, which validated its identity. Cell stocks were frozen upon arrival and subcultured fewer than four times before being discarded. ARPE19 cells were grown in Dulbecco's modified Eagle's medium/F12 (50/50) media supplemented with 10% fetal bovine serum and 1% Pen-Strep. THP-1 cells were grown in RPMI-1640 supplemented with 10% fetal bovine serum and 1% Pen-Strep. All the cell cultures were maintained in an incubator at 37 °C with 5% CO_2. All stable cell lines generated by lentiviral vector transduction were grown in the corresponding media supplemented with puromycin at a dose of 1 μg/ml.

Transfection. Cells were plated at 8×10^5 cells per well in a six-well plate with complete growth medium and incubated for 24 hours. The next day, complete growth medium was replaced in each well with 2 ml of serum- and antibiotic-free medium. Plasmid DNA complexes were generated by diluting 4 μg of the corresponding DNA in 100 μl of sterile phosphate-buffered saline (PBS) and 10 μg of a 1 μg/μl of polyethyleneimine[49] (PEI) in 100 μl of PBS. Dilutions were incubated at room temperature for 5 minutes. DNA:PEI complexes were made by mixing the diluted DNA and PEI and incubating them for 20 minutes at room temperature. Complexes were overlaid on the cells drop wise and cells were maintained at 37 °C for 18 hours. The transfection was stopped by removing the complex-containing medium and replacing it with 3 ml of complete growth medium. Cells were

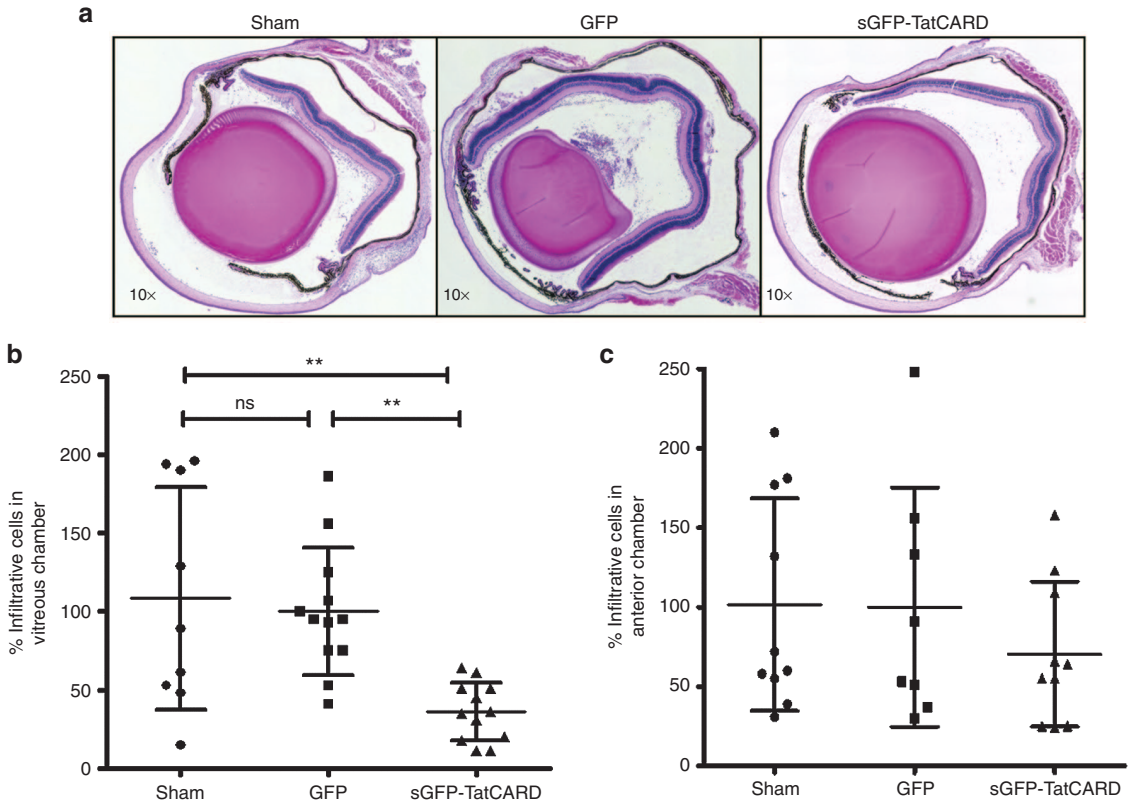

Figure 6 Expression of the TatCARD gene product reduces cellular infiltration observed in the endotoxin-induced uveitis mouse model. (**a**) Representative histological differences between eyes injected with GFP and eyes injected with sGFP-TatCARD. Eyes were enucleated 24 hours post-lipopolysaccharide injection, fixed, embedded, sectioned, and stained with hematoxylin and eosin. Pictures were taken with a light microscope at original magnifications of 5× and 10×. (**b**) Expression of the TatCARD gene results in a 64% reduction in the number of infiltrating cells within the vitreous. The number of infiltrating cells was divided by the average number of infiltrating cells per section in the GFP-treated eye (616 cells) and multiplied by 100 to obtain the percentage values. Values represent average ± SD, $n = 9$ sham-injected eyes, $n = 12$, GFP- and TatCARD-injected eyes. (**c**) Expression of the TatCARD gene does not affect the number of infiltrating cells within the anterior chamber. The numbers of infiltrating cells within the anterior chamber were quantified and the absolute numbers standardized to the average number of cells in the GFP-treated eye (206 cells). Values represent average ± SD, $n = 10$; sham and TatCARD eyes, $n = 8$ GFP eyes). CARD, caspase activation and recruitment domain.

grown for another 24 hours at 37 °C. Afterwards, cells were harvested by trypsin treatment and centrifugation.

Viral vectors. All the lentiviral vectors were created using the pCDH-EF1-MCS-T2A-Puro plasmid (Systems Biosciences, Mountain View, CA). The transgenes were cloned using the EcoRI and the NotI restriction sites in the multiple cloning sites. Plasmids were grown in DH5α cells and sequenced by the Sanger method. To generate viral particles, the plasmids were cotransfected with the pPACKH1 lentivector packaging kit (Systems Biosciences) in HEK293T cells. The lentiviral vector–containing media were harvested at 48 hours after the cotransfection and were pelleted by centrifugation at 2,560 ×*g* for 5 minutes at 4 °C. The vector-containing media were filtered using a 0.22-µm syringe filter.

AAV vectors were designed by cloning the corresponding gene of interest between the inverted terminal repeats of the AAV present in the plasmid. Once verified by the Sanger method of DNA sequencing, this plasmid was propagated in Sure 2 cells (Agilent Technologies, Santa Clara, CA). The presence of intact inverted terminal repeats was determined by XmaI digestion at 37 °C for 2 hours. Large-scale DNA was prepared by CsCl purification of DNA before packaging as viral particles. Finally, AAV viral particles were generated, purified, and titrated by the Vector Core of the Center for Vision Research at the University of Florida.

Immunoprecipitation. ARPE-19 cells expressing either TatCARD or only the puromycin resistance gene were disrupted in NP-40 lysis buffer (1% NP-40, 150 mmol/l NaCl, 50 mmol/l Tris-Cl pH 8.0) supplemented with Protease Inhibitors Cocktail (Thermo Fisher Scientific, Rockford, IL) and 2 mmol/l ethylenediaminetetraacetic acid. Samples were kept on ice for 20 minutes and mixed by vortexing every ten minutes followed by a centrifugation at 16,000 × g for 15 minutes at 4 °C. Lysate was collected, and the protein concentration was measured with the DC Protein Assay (Bio-Rad, Hercules, CA) according to the manufacturer's protocol. Lysates were diluted to 1 µg/µl. A total of 500 µg of lysate was incubated with 1 µg of normal rabbit IgG antibody (Santa Cruz Biotechnology, Dallas, TX) and 20-µl protein A/G-agarose beads (Santa Cruz Biotechnology) at 4 °C for 1 hour in a rotating mixer. Beads were pelleted by centrifugation at 1,000 × g for 5 minutes at 4 °C. A total of 5 µg of anti-caspase-1 antibody (Millipore, Billerica, MA) were added to 20 µg protein A/G-agarose beads in a total volume of 500 µl PBS and were incubated at 4 °C for 1 hour in a rotating mixer. Antibody/bead complex was pelleted by centrifugation as done previously and was resuspended in 500 µl of 0.2 mol/l triethanolamine pH 8.3 containing 20 mmol/l of the cross-linking agent dimethyl pimelimidate (Sigma-Aldrich, St Louis MO). The complexes were incubated for 1 hour at room temperature in a rotating mixer. The cross-linking reaction was quenched by adding 50 µl of 1 mol/l Tris-HCl pH 7.5 and incubating for 1 hour at room temperature in a rotating mixer. The complexes were pelleted by centrifuging as done previously. The complexes were washed with 500 µl of 0.2 mol/l glycine HCl pH 2.5 by incubating them for 1 minute at room temperature in a rotating mixer. These complexes were then washed three times with PBS containing 0.01% Tween-20. A total of 500 µl of diluted lysate (500 µg protein) was used to resuspend the pellet. Samples were kept at 4 °C overnight in a rotating mixer. The next day, samples were

centrifuged at 1,000 × g for 5 minutes at 4 °C. Supernatant was removed and the pellet was washed four times with NP-40 lysis buffer by resuspending and centrifuging as in previous steps. After the last wash, the pellet was resuspended in 60 µl of Laemmli sample buffer and boiled for 5 minutes. Samples were centrifuged at 16,000 × g for 10 seconds, and supernatants were transferred to new 1.5 ml microcentrifuge tubes. A total of 20 µl of sample were analyzed in a 12% SDS polyacrylamide gel and transferred onto PVDF membranes using the iBlot system. Membranes were probed with anti-Caspase-1 (Millipore, 1:1,000 dilution) or anti-T2A (Millipore, 1:1,000 dilution).

Enzyme-linked immunosorbent assay. Medium was harvested from the indicated cultures and 100 µl aliquots were used to quantify IL-1β concentration. The enzyme-linked immunosorbent assay kit for the human IL-1β was purchased from Ray Biotech (Norcross, GA). The enzyme-linked immunosorbent assay kit for the human IL-18 was purchased from eBioscience (San Diego, CA). The concentration of these cytokines was determined according to the manufacturer's protocol.

Western blot. Cells were disrupted as described above. Protein lysates were diluted in Laemmli sample buffer containing 100 µmol/l DTT and boiled for 5 minutes. Equal amounts of protein were separated by SDS polyacrylamide gel electrophoresis and transferred into a PVDF membrane using the iBlot system (Invitrogen, Grand Island, NY). This membrane was blocked with a proprietary blocking buffer from Li-Cor (Li-Cor Biosciences, Lincoln, Nebraska) for 1 hour at room temperature and incubated overnight with the designated primary antibody at 4 °C. The next day, the primary antibody was discarded and the membrane was washed three times with PBS-T (1× PBS with 0.1% Tween 20) at a rate of 5 minutes per wash. To detect the primary antibody, the corresponding secondary antibody conjugated with an IR-Dye (Li-Cor Biosciences, Lincoln, Nebraska) was diluted 1:5,000 with proprietary blocking buffer supplemented with 0.1% Tween 20. After the last wash, the membrane was incubated with the diluted secondary antibody and incubated at room temperature with constant shaking for 45 minutes. Finally, the membrane was washed four times with PBS-T as described before and then was scanned using a Li-Cor Odyssey Scanner.

EIU mouse model. Animal experiments were reviewed and approved by the University of Florida Institutional Animal Care and Use Committee. Mice of the C57B/6 strain were anesthetized with ketamine and xylazine and injected in the vitreous of each eye with 3×10^9 vector genomes of AAV2(quadY-F+T-V) expressing either GFP or sGFP-TatCARD from the CMV enhancer-chicken β-actin promoter. As a control for the effects of the injection, a group of mice were sham injected with sterile saline. The injections were performed through the limbus of the anesthetized animals without paracentesis. Mice received topical antibiotics after the procedure to prevent infections at the site of incision. One month after the injection, GFP expression was observed by fluorescent fundoscopy. The next day, mice were injected intravitreally in each eye with 25 ng of LPS. After 24 hours, these mice were sacrificed by inhalation with CO_2 followed by thoracotomy, and their eyes were enucleated and placed in 4% paraformaldehyde at 4 °C overnight. Eyes were embedded in paraffin were sectioned through the cornea-optic nerve axis at a thickness of 12 µm. The sections were collected in independent slides with sections on the same slide having a difference of 96 µm. Slides were stained with hematoxylin and eosin to visualize infiltrating cells. These cells were counted in images of the sections by two independent masked observers. At least two noncontinuous sections from each slide were quantified by each observer, with no section being counted by both observers.

Isolation of vitreous. Vitreous was isolated using the protocol reported by Skeie *et al.*[50] Briefly, mice were euthanized using CO_2 as described above. A transverse incision was made in the cornea with a surgical scalpel to allow the aqueous humor to flow. Excess aqueous humor was absorbed with a paper towel. The retina, vitreous, and lens were eviscerated by squeezing the eye from the back. Tissues were collected into a sterile 1.5-ml tube and later transferred into an Amicon Ultra Centrifugal Filter with a cut off membrane of 50 KDa (EMD Millipore). An additional 100 µl of PBS supplemented with Protease Inhibitors Cocktail (Thermo Fisher Scientific, Rockford, IL) was added to the tube. Samples were centrifuged at 14,000 × g for 15 minutes, and vitreous flow trough was collected. Protein concentration of the vitreous was determined by DC Assay as described previously and stored at −20 °C until assayed.

Fundoscopy, ERG and SD-OCT. We used digital fundus imaging with a Micron III retinal imaging microscope (Phoenix Research Laboratories, Pleasaton, CA) to monitor gene expression by fluorescence. Conscious mice had their eyes dilated with 1% atropine and 10% phenylephrine. Mice were then anesthetized with a mixture of ketamine and xylazine in normal saline. To avoid loss of moisture from the ocular surface during the procedure, mice received a drop of 2.5% hypermellose ophthalmic demulcent solution (Gonak, AKORN, Lake Forest, IL). Using the fluorescein filters, we detect GFP fluorescence using the same exposure time for all the eyes. ERG and SD-OCT analyses were performed as described earlier.[49]

Statistical analysis. Statistical analysis was performed using the Prism 5 software (GraphPad, San Diego, CA). For all *in vitro* studies, averages of replicate experiments were compared by analysis of variance followed by the Newman-Keuls test to detect differences among all groups. For *in vivo* studies, the Kruskal-Wallis test followed by the Dunn's multiple comparison test were used to avoid biases caused by potential outliers. Statistical significance was reported whenever the calculated P value was ≤ 0.05. $^*P$ value ≤ 0.05, $^{**}P$ value ≤ 0.01, $^{***}P$ value ≤ 0.001.

ACKNOWLEDGMENTS

We would like to acknowledge the technical help of James Thomas Jr. for the production of DNA and Vince Chiodo at the Center for Vision Research Vector Core for the production of the AAV vectors. We would also like to acknowledge the help of Zhaoyang Wang and Brian Rossmiller with the animal injections. Finally, we would like to thank Chulbul Ahmed for his insightful review of this manuscript. This research was funded by a grant from the National Eye Institute (R01 EY02025), a grant from the Florida Biomedical Research Foundation (e-10KG-s), an AMD Research Fellowship from ARVO/Genentech, and from the Shaler Richardson Professorship endowment. Core facilities were supported by NEI grant P30 EY02172.

REFERENCES

1. Patel, JI, Saleh, GM, Hykin, PG, Gregor, ZJ and Cree, IA (2008). Concentration of haemodynamic and inflammatory related cytokines in diabetic retinopathy. *Eye (Lond)* **22**: 223–228.
2. Tseng, WA, Thein, T, Kinnunen, K, Lashkari, K, Gregory, MS, D'Amore, PA *et al.* (2013). NLRP3 inflammasome activation in retinal pigment epithelial cells by lysosomal destabilization: implications for age-related macular degeneration. *Invest Ophthalmol Vis Sci* **54**: 110–120.
3. Mo, J-S, Matsukawa, A, Ohkawara, S and Yoshinaga, M (1998). Involvement of TNF α, IL-1β and IL-1 receptor antagonist in LPS-induced rabbit uveitis. *Exp Eye Res* **66**: 547–557.
4. Latz, E, Xiao, TS and Stutz, A (2013). Activation and regulation of the inflammasomes. *Nat Rev Immunol* **13**: 397–411.
5. Wen, H, Miao, EA and Ting, JP (2013). Mechanisms of NOD-like receptor-associated inflammasome activation. *Immunity* **39**: 432–441.
6. Zhong, Y, Kinio, A and Saleh, M (2013). Functions of NOD-Like Receptors in Human Diseases. *Front Immunol* **4**: 333.
7. Yego, EC, Vincent, JA, Sarthy, V, Busik, JV and Mohr, S (2009). Differential regulation of high glucose-induced glyceraldehyde-3-phosphate dehydrogenase nuclear accumulation in Müller cells by IL-1beta and IL-6. *Invest Ophthalmol Vis Sci* **50**: 1920–1928.
8. Shi, G, Maminishkis, A, Banzon, T, Jalickee, S, Li, R, Hammer, J *et al.* (2008). Control of chemokine gradients by the retinal pigment epithelium. *Invest Ophthalmol Vis Sci* **49**: 4620–4630.
9. Aveleira, C, Castilho, A, Baptista, F, Simões, N, Fernandes, C, Leal, E *et al.* (2010). High glucose and interleukin-1beta downregulate interleukin-1 type I receptor (IL-1RI) in retinal endothelial cells by enhancing its degradation by a lysosome-dependent mechanism. *Cytokine* **49**: 279–286.
10. Dinarello, CA and van der Meer, JW (2013). Treating inflammation by blocking interleukin-1 in humans. *Semin Immunol* **25**: 469–484.
11. Goh, AX, Bertin-Maghit, S, Ping Yeo, S, Ho, AW, Derks, H, Mortellaro, A *et al.* (2014). A novel human anti-interleukin-1β neutralizing monoclonal antibody showing *in vivo* efficacy. *MAbs* **6**: 765–773.

12. Movva, R, Brown, SB, Morris, DL and Figueredo, VM (2013). Anakinra for myocarditis in juvenile idiopathic arthritis. *Tex Heart Inst J* **40**: 623–625.
13. Planck, SR, Woods, A, Clowers, JS, Nicklin, MJ, Rosenbaum, JT and Rosenzweig, HL (2012). Impact of IL-1 signalling on experimental uveitis and arthritis. *Ann Rheum Dis* **71**: 753–760.
14. Lalor, SJ, Dungan, LS, Sutton, CE, Basdeo, SA, Fletcher, JM and Mills, KH (2011). Caspase-1-processed cytokines IL-1beta and IL-18 promote IL-17 production by gammadelta and CD4 T cells that mediate autoimmunity. *J Immunol* **186**: 5738–5748.
15. Siegmund, B, Fantuzzi, G, Rieder, F, Gamboni-Robertson, F, Lehr, HA, Hartmann, G *et al.* (2001). Neutralization of interleukin-18 reduces severity in murine colitis and intestinal IFN-gamma and TNF-alpha production. *Am J Physiol Regul Integr Comp Physiol* **281**: R1264–R1273.
16. Ten Hove, T, Corbaz, A, Amitai, H, Aloni, S, Belzer, I, Graber, P *et al.* (2001). Blockade of endogenous IL-18 ameliorates TNBS-induced colitis by decreasing local TNF-alpha production in mice. *Gastroenterology* **121**: 1372–1379.
17. Banda, NK, Vondracek, A, Kraus, D, Dinarello, CA, Kim, SH, Bendele, A *et al.* (2003). Mechanisms of inhibition of collagen-induced arthritis by murine IL-18 binding protein. *J Immunol* **170**: 2100–2105.
18. Raeburn, CD, Dinarello, CA, Zimmerman, MA, Calkins, CM, Pomerantz, BJ, McIntyre, RC Jr *et al.* (2002). Neutralization of IL-18 attenuates lipopolysaccharide-induced myocardial dysfunction. *Am J Physiol Heart Circ Physiol* **283**: H650–H657.
19. Woldbaek, PR, Sande, JB, Strømme, TA, Lunde, PK, Djurovic, S, Lyberg, T *et al.* (2005). Daily administration of interleukin-18 causes myocardial dysfunction in healthy mice. *Am J Physiol Heart Circ Physiol* **289**: H708–H714.
20. Rosenbaum, JT and Kim, HW (2013). Innate immune signals in autoimmune and autoinflammatory uveitis. *Int Rev Immunol* **32**: 68–75.
21. Yadav, UCS and Ramana, KV (2013). Endotoxin-induced uveitis in rodents. In: Allen IC (ed.). *Mouse Models Innate Immun*. Humana Press, Springer Verlag, Berlin. pp 155–162. <http://link.springer.com/protocol/10.1007/978-1-62703-481-4_18>.
22. Xu, Y, Chen, W, Lu, H, Hu, X, Li, S, Wang, J *et al.* (2010). The expression of cytokines in the aqueous humor and serum during endotoxin-induced uveitis in C3H/HeN mice. *Mol Vis* **16**: 1689–1695.
23. Planck, SR, Becker, MD, Crespo, S, Choi, D, Galster, K, Garman, KL *et al.* (2008). Characterizing extravascular neutrophil migration *in vivo* in the iris. *Inflammation* **31**: 105–111.
24. Silhol, M, Tyagi, M, Giacca, M, Lebleu, B and Vivès, E (2002). Different mechanisms for cellular internalization of the HIV-1 Tat-derived cell penetrating peptide and recombinant proteins fused to Tat. *Eur J Biochem* **269**: 494–501.
25. Kauppinen, A, Niskanen, H, Suuronen, T, Kinnunen, K, Salminen, A and Kaarniranta, K (2012). Oxidative stress activates NLRP3 inflammasomes in ARPE-19 cells–implications for age-related macular degeneration (AMD). *Immunol Lett* **147**: 29–33.
26. Tang, SC, Lathia, JD, Selvaraj, PK, Jo, DG, Mughal, MR, Cheng, A *et al.* (2008). Toll-like receptor-4 mediates neuronal apoptosis induced by amyloid beta-peptide and the membrane lipid peroxidation product 4-hydroxynonenal. *Exp Neurol* **213**: 114–121.
27. Verma, A, Shan, Z, Lei, B, Yuan, L, Liu, X, Nakagawa, T *et al.* (2012). ACE2 and Ang-(1-7) confer protection against development of diabetic retinopathy. *Mol Ther* **20**: 28–36.
28. Boye, SE, Boye, SL, Lewin, AS and Hauswirth, WW (2013). A comprehensive review of retinal gene therapy. *Mol Ther* **21**: 509–519.
29. Beltran, WA, Boye, SL, Boye, SE, Chiodo, VA, Lewin, AS, Hauswirth, WW *et al.* (2010). rAAV2/5 gene-targeting to rods:dose-dependent efficiency and complications associated with different promoters. *Gene Ther* **17**: 1162–1174.
30. Kay, CN, Ryals, RC, Aslanidi, GV, Min, SH, Ruan, Q, Sun, J *et al.* (2013). Targeting photoreceptors via intravitreal delivery using novel, capsid-mutated AAV vectors. *PLoS One* **8**: e62097.
31. Chen, FT, Liu, YC, Yang, CM and Yang, CH (2012). Anti-inflammatory effect of the proteasome inhibitor bortezomib on endotoxin-induced uveitis in rats. *Invest Ophthalmol Vis Sci* **53**: 3682–3694.
32. Allen, JB, McGahan, MC, Ferrell, JB, Adler, KB and Fleisher, LN (1996). Nitric oxide synthase inhibitors exert differential time-dependent effects on LPS-induced uveitis. *Exp Eye Res* **62**: 21–28.
33. Guex-Crosier, Y, Wittwer, AJ and Roberge, FG (1996). Intraocular production of a cytokine (CINC) responsible for neutrophil infiltration in endotoxin induced uveitis. *Br J Ophthalmol* **80**: 649–653.
34. Hayashi, S, Guex-Crosier, Y, Delvaux, A, Velu, T and Roberge, FG (1996). Interleukin 10 inhibits inflammatory cells infiltration in endotoxin-induced uveitis. *Graefes Arch Clin Exp Ophthalmol* **234**: 633–636.
35. Jin, H, Yang, X, Liu, K, Gu, Q and Xu, X (2011). Effects of a novel peptide derived from human thrombomodulin on endotoxin-induced uveitis *in vitro* and in vivo. *FEBS Lett* **585**: 3457–3464.
36. Kubota, S, Kurihara, T, Mochimaru, H, Satofuka, S, Noda, K, Ozawa, Y *et al.* (2009). Prevention of ocular inflammation in endotoxin-induced uveitis with resveratrol by inhibiting oxidative damage and nuclear factor-kappaB activation. *Invest Ophthalmol Vis Sci* **50**: 3512–3519.
37. Lajavardi, L, Bochot, A, Camelo, S, Goldenberg, B, Naud, MC, Behar-Cohen, F *et al.* (2007). Downregulation of endotoxin-induced uveitis by intravitreal injection of vasoactive intestinal Peptide encapsulated in liposomes. *Invest Ophthalmol Vis Sci* **48**: 3230–3238.
38. Tsai, M-L, Horng, C-T, Chen, S-L, Xiao, X, Wang, C-H and Tsao, Y-P (2009). Suppression of experimental uveitis by a recombinant adeno-associated virus vector encoding interleukin-1 receptor antagonistat. <http://www.molvis.org/molvis/v15/a165/>.
39. Rosenzweig, HL, Woods, A, Clowers, JS, Planck, SR and Rosenbaum, JT (2012). The NLRP3 inflammasome is active but not essential in endotoxin-induced uveitis. *Inflamm Res* **61**: 225–231.
40. Zheng, TS, Hunot, S, Kuida, K, Momoi, T, Srinivasan, A, Nicholson, DW *et al.* (2000). Deficiency in caspase-9 or caspase-3 induces compensatory caspase activation. *Nat Med* **6**: 1241–1247.
41. Miao, EA, Rajan, JV and Aderem, A (2011). Caspase-1-induced pyroptotic cell death. *Immunol Rev* **243**: 206–214.
42. Perche, O, Doly, M and Ranchon-Cole, I (2007). Caspase-dependent apoptosis in light-induced retinal degeneration. *Invest Ophthalmol Vis Sci* **48**: 2753–2759.
43. Samardzija, M, Wenzel, A, Thiersch, M, Frigg, R, Remé, C and Grimm, C (2006). Caspase-1 ablation protects photoreceptors in a model of autosomal dominant retinitis pigmentosa. *Invest Ophthalmol Vis Sci* **47**: 5181–5190.
44. Kowluru, RA, Mohammad, G, Santos, JM, Tewari, S and Zhong, Q (2011). Interleukin-1β and mitochondria damage, and the development of diabetic retinopathy. *J Ocul Biol Dis Infor* **4**: 3–9.
45. Liu, Y, Biarnés Costa, M and Gerhardinger, C (2012). IL-1β is upregulated in the diabetic retina and retinal vessels: cell-specific effect of high glucose and IL-1β autostimulation. *PLoS One* **7**: e36949.
46. Tarallo, V, Hirano, Y, Gelfand, BD, Dridi, S, Kerur, N, Kim, Y *et al.* (2012). DICER1 loss and Alu RNA induce age-related macular degeneration via the NLRP3 inflammasome and MyD88. *Cell* **149**: 847–859.
47. Lavalette, S, Raoul, W, Houssier, M, Camelo, S, Levy, O, Calippe, B *et al.* (2011). Interleukin-1β inhibition prevents choroidal neovascularization and does not exacerbate photoreceptor degeneration. *Am J Pathol* **178**: 2416–2423.
48. Mao, H, Seo, SJ, Biswal, MR, Li, H, Conners, M, Nandyala, A *et al.* (2014). Mitochondrial oxidative stress in the retinal pigment epithelium leads to localized retinal degeneration. *Invest Ophthalmol Vis Sci* **55**: 4613–4627.
49. Reed, SE, Staley, EM, Mayginnes, JP, Pintel, DJ and Tullis, GE (2006). Transfection of mammalian cells using linear polyethylenimine is a simple and effective means of producing recombinant adeno-associated virus vectors. *J Virol Methods* **138**: 85–98.
50. Skeie, JM, Tsang, SH and Mahajan, VB (2011). Evisceration of mouse vitreous and retina for proteomic analyses. *J Vis Exp* **50**: 2795.